JVI Journals.ASM.org

Reassortment Complements Spontaneous Mutation in Influenza A Virus NP and M1 Genes To Accelerate Adaptation to a New Host

William L. Ince, Aissatou Gueye-Mbaye, Jack R. Bennink, Jonathan W. Yewdell

Laboratory of Viral Diseases, National Institute of Allergy and Infectious Diseases, Bethesda, Maryland, USA

Influenza A virus (IAV) infects a remarkably wide variety of avian and mammalian hosts. Evolution finely hones IAV genes to optimally infect and be transmitted in a particular host species. Sporadically, IAV manages to jump between species, introducing novel antigenic strains into the new host population that wreak havoc until herd immunity develops. IAV adaptation to new hosts typically involves reassortment of IAV gene segments from coinfecting virus strains adapted to different hosts in conjunction with multiple adaptive mutations in the various IAV genes. To better understand host adaptation between mammalian species in real time, we passaged mouse-adapted A/PR8/34 (PR8) in guinea pigs. Guinea pigs, unlike mice, support spontaneous and robust IAV transmission. For some IAV strains, including PR8, adaptation is required for a virus to attain transmissibility, providing an opportunity to understand the evolution of transmissibility in guinea pigs. Multiple guinea pig-adapted PR8 mutants generated by serial nasal wash passaging in independent lines replicated more efficiently and were transmitted by cocaging. All transmissible variants possessed one of two nonsynonymous mutations in M1, either alone or in combination with mutations in PB2, HA, NP, or NA. Rapid reassortment between independently selected variants combined beneficial mutations in NP and M1 to form the fittest virus capable of being transmitted. These findings provide further insight into genetic determinants in NP and M1 involved in PR8 IAV adaptation to be transmitted in a new host and clearly show the benefit of a segmented genome in rapidly generating optimal combinations of mutations in IAV evolution.

Influenza A virus (IAV) remains an important human pathogen due to its antigenic variability. IAV provides a constantly moving target for the humoral immune system due to gradual antigenic evolution (antigenic drift) and abrupt shifts in antigenicity (antigenic shift). Antigenic shift results from the remarkable ability of IAV to adapt to a wide variety of avian and mammalian hosts, which creates genetically distinct reservoirs from which antigenically novel variants can invade the human population and cause devastating pandemics.

While avian species harbor the largest and most diverse IAV populations (1–3), viruses replicating in mammals historically pose the most immediate threat to humans (4). This was recently demonstrated by the 2009 swine origin H1N1 IAV pandemic (pH1N1) (5). Two key features of IAV enhance its adaptability. First, its segmented genome enables rapid reassortment of the 8 gene segments encoding the 13 defined gene products (6, 7). Reassortment plays a central role in IAV evolution, particularly in host adaptation, in which invading virus strains can rapidly acquire host-optimized alleles from the endemic virus. For example, swine, which are permissive to many avian and human viruses, can generate reassortant viruses with antigenically novel avian glycoproteins combined with internal genes adapted for replication in mammals (3, 4). Second, a mutation rate just below the catastrophe limit (8) allows IAV to rapidly sample the available mutation space to optimize viral replication in new hosts as well as generate immune escape variants.

Different *in vivo* models of influenza virus infection provide unique views of IAV evolution (9). Viral determinants of host adaptation and pathogenicity have been studied extensively in mice and ferrets using forward and reverse genetics approaches (reviewed in references 10, 11, and 12). Guinea pigs (GPs) support replication and transmission of a wide variety of influenza viruses and have been increasingly utilized as a relatively low-cost alternative to the ferret transmission model (13–15). Here, we explore the evolution of mouse-adapted IAV as it adapts to propagate and be transmitted in the GP.

MATERIALS AND METHODS

Viruses. A/Puerto Rico/8/1934 (PR8) was generated using an 8-plasmid molecular clone rescue system (16) (GenBank accession numbers AF389115 to AF389122), generously contributed by Adolfo Garcia-Sastre. This clone differs from the published sequence (above) at two positions: PB1 A549C (K175N) and HA A651C (I207L) (H1 numbering). We generated seed virus by transfecting 293T cells with the 8-plasmid molecular clone. Output virus was then expanded once in Madin-Darby canine kidney (MDCK) cells and then in embryonated chicken eggs. Molecular-clone-derived mutants were generated using site-directed mutagenesis as described previously (17). All molecular-clone-derived viruses were expanded on MDCK cells in Gibco minimal essential medium (MEM) with GlutaMAX (Life Technologies, Grand Island, NY) supplemented with 1 μg/ml of tosylsulfonyl phenylalanyl chloromethyl ketone (TPCK)-treated trypsin. All tissue culture and nasal wash-derived virus titers were determined by endpoint dilution on MDCK cells, and the 50% tissue culture infective doses ($TCID_{50}$s) were determined using the Reed-Muench method. Virus plaques were prepared on MDCK monolayers under an agarose overlay as previously described (18).

Infections and passaging. We conducted research in compliance with the PHS policy, Office of Laboratory Animal Welfare (OLAW), guidance and all guidelines of the NIAID Institutional Animal Care and Use Committee (IACUC). Research was conducted under a protocol approved by the NIAID IACUC. Specific-pathogen-free female Hartley strain GPs were obtained from Charles River Laboratories (Frederick, MD). Animals

Received 2 October 2012 Accepted 26 January 2013
Published ahead of print 30 January 2013
Address correspondence to Jonathan W. Yewdell, JYEWDELL@niaid.nih.gov.

doi:10.1128/JVI.02749-12

TABLE 1 Reassortment and relative fitness of the AB20- and A10-derived genotypes in a competition experiment

Virus population[a]	All reassortants (%)	Reassortants with unlinked NP/M (%)	Relative fitness[b] of $NP_{F346S}/M1_{V166\ M}$	n[d]
GP1A	16	5	1.6	30
GP2A	0	0	>1.52[c]	22
GP3A	28	18	1.45	22
GP1B	36	19	1.41	21
GP2B	16	11	>1.32[c]	19
GP3B	43	23	1.49	23

[a] Virus populations described in Fig. 5.
[b] Relative fitness based on input and 48h NW sample frequencies (see Materials and Methods) of genotypes containing AB20-derived NP_{F346S} and $M1_{V166\ M}$ alleles versus those containing the A10 NP and M1 alleles.
[c] For GP2A and GP2B, minimum-fitness estimations were based on the maximum frequency of the unsampled A10 NP/M1 variant (3/N).
[d] Number of plaque-cloned viruses used for the analysis.

used in all experiments were age matched and from the same cohort, which ranged from 5 to 12 weeks old. For infections, guinea pigs were anesthetized by isoflurane inhalation and infected intranasally (i.n.) with the $TCID_{50}$s indicated below in 300 μl of balanced salt solution containing 0.1% bovine serum albumin (BSA). Nasal washes were collected from isoflurane-anesthetized GPs by inserting 1 ml of phosphate-buffered saline, supplemented with 100 U/ml of penicillin and 100 μg/ml of streptomycin, into one nostril while flowthrough was collected from the opposite nostril.

We initiated GP passage lines by intranasal infection with an egg stock of the molecular-clone-derived PR8 and maintained virus in GPs in parallel using age-matched animals from the same purchased cohort. In passages 1 to 10, animals 8 to 12 weeks old (mode = 8 weeks old) were used. In passages 11 to 20, animals 5 to 10 weeks old (mode = 6 weeks old) were used. Nasal wash samples taken at 48 h postinfection were either aliquoted, flash frozen on dry ice, and stored at −80°C or used immediately to inoculate the succeeding guinea pig and then flash frozen for further analysis. Aliquots from frozen samples were used to continue passage lines when necessary. In the first 5 passages, 300 μl of undiluted nasal wash was used for inoculations. Thereafter, 30 μl of nasal wash was diluted 1:10 in 270 μl of balanced salt solution (BSS) containing 0.1% BSA and used for infections.

Transmission experiments. We performed transmission experiments under the controlled ambient humidity and temperature conditions in the vivarium. Relative humidity and temperature for all experiments ranged from 42 to 62% and 21 to 22.8°C (median values, 54% and 22°C). Animals from the same cohort were used in individual experiments. Ages of cohorts ranged from 5 to 8 weeks (mode = 6.5 weeks). Recipient animals were cocaged with donor animals at 24 h postinfection and were monitored for infection by nasal wash at the frequencies indicated below. All statistical analyses were performed using Prism 5 (Graphpad, La Jolla, CA).

Calculation of relative fitness. For the competition experiment analysis illustrated in Table 1, variant frequencies were estimated by sequencing plaque-cloned viruses. We calculated relative fitness (w) of the $PR8_{gpAB20}$-derived genotypic variants using the following equation:

$$\log\left(\frac{p_t}{q_t}\right) = \log\left(\frac{p_0}{q_0}\right) + t\log(w)$$

where p and q are frequencies of the $PR8_{gpAB20}$- and $PR8_{gpA10}$-derived variants in the input sample (0) and at 48 h postinfection (t). Here, $t = 6$ generations (assuming 8 h/generation).

RT-PCR and sequencing. RNA was extracted from tissue culture and biological samples using a QiaAmp viral RNA minikit (Valencia, CA) and was reverse transcribed using a minus-strand-specific universal primer mix (5′-AGCRAAAGCAGG-3′) and an Abgene Verso reverse transcription-PCR (RT-PCR) kit (Thermo Scientific, Rockford, IL). PCR was performed using Platinum *Taq* HiFi DNA polymerase (Invitrogen Life Technologies, Grand Island, NY) with segment-specific or universal influenza virus primers described elsewhere (19). PCR samples were sequenced using specific primers (sequences available upon request) for each segment and processed for Sanger sequencing using BigDye Terminator technology (Invitrogen Life Technologies) and run on an ABI 3730xl sequencer.

RESULTS

Adaptation of PR8 to GPs by serial passaging. A/Puerto Rico/8/1934 (PR8) has been extensively passaged in mice, eggs, and cultured cells over its long history (20, 21). In contrast to A/California/04/2009 (CAL), which, like other human isolates, replicates to high titers and is transmitted well between GPs (22–24), PR8 fails to be transmitted between cocaged animals (Fig. 1A and B). Compared to CAL, PR8 exhibits over a 100-fold reduction in average nasal wash titer at 48 h postinfection (p.i.) and reaches a 10-fold-lower mean peak titer, which is delayed by 48 h (Fig. 1E and F). PR8 therefore provides an opportunity to characterize IAV adaptive evolution in a new host.

We passaged a molecular-clone-derived PR8 virus ($PR8_{WT}$) through 10 serial GP nasal wash infections in two separate lines ($PR8_{gpAn}$ and $PR8_{gpBn}$, where n = number of passages), which were then combined ($PR8_{gpABn}$) and passaged for an additional 10 rounds. We initiated passages $PR8_A$ and $PR8_B$ with 10^5 and 10^6 $TCID_{50}$s, respectively. In the 5 initial rounds, the minimum input passaging doses for $PR8_{gpA}$ and $PR8_{gpB}$ were 3.5×10^4 and 5×10^3 $TCID_{50}$s, with respective median doses of 10^5 and 5×10^5 $TCID_{50}$s. In subsequent passages, to maximize viral replication, we decreased the input 10-fold for each passage line, using between 1.6×10^3 and 5×10^3 $TCID_{50}$s for infection. At these doses, mutants representing >0.2% or >0.06%, respectively, of the donor population could reasonably be expected (95% confidence) to be sampled for the next round of infection (25), thus limiting the severity of the interpassage bottleneck.

Increased replication kinetics and transmissibility of GP-adapted PR8. After their initial 10 independent passages, we assessed the replication kinetics of $PR8_{gpA10}$ and $PR8_{gpB10}$ and their ability to be transmitted between cocaged GPs. A naïve recipient GP was cocaged 1 to 1 with each of 3 donors intranasally infected with $PR8_{gpA10}$ or $PR8_{gpB10}$ viruses. Both $PR8_{gpA10}$ (3 of 3) and $PR8_{gpB10}$ (2 of 3) were transmitted to naïve cage mates (Fig. 1C and D), indicating that PR8 was adapting rapidly to its new host. Animals infected with $PR8_{gpA10}$ and $PR8_{gpB10}$ viruses showed a 2- to 3-log_{10} increase in nasal wash titers at 48 h compared to animals infected with $PR8_{WT}$ (Fig. 1E) and also reached peak virus titer earlier than $PR8_{WT}$-infected GPs (Fig. 1F). We could detect no significant differences in replication kinetics or transmission rates between $PR8_{gpA10}$ and $PR8_{gpB10}$ viruses (Fig. 1C to F), indicating that the two lines were similarly adapted to GPs.

M1 mutations are rapidly selected during GP adaptation. Bulk genomic sequencing of selected $PR8_{gpA}$ and $PR8_{gpB}$ passages demonstrated that increased replication kinetics and transmissibility were accompanied by nonsynonymous substitutions in multiple genes (Fig. 2). Interestingly, the earliest detectable substitutions were clearly present by passage 3, $M1_{F62L}$ in $PR8_{gpA}$ and $M1_{V166M}$ in $PR8_{gpB}$, each reaching 100% by passage 5 and stable thereafter (Fig. 2A to F). Their rapid independent emergence in each line suggests relatively strong selection for substitutions in M1.

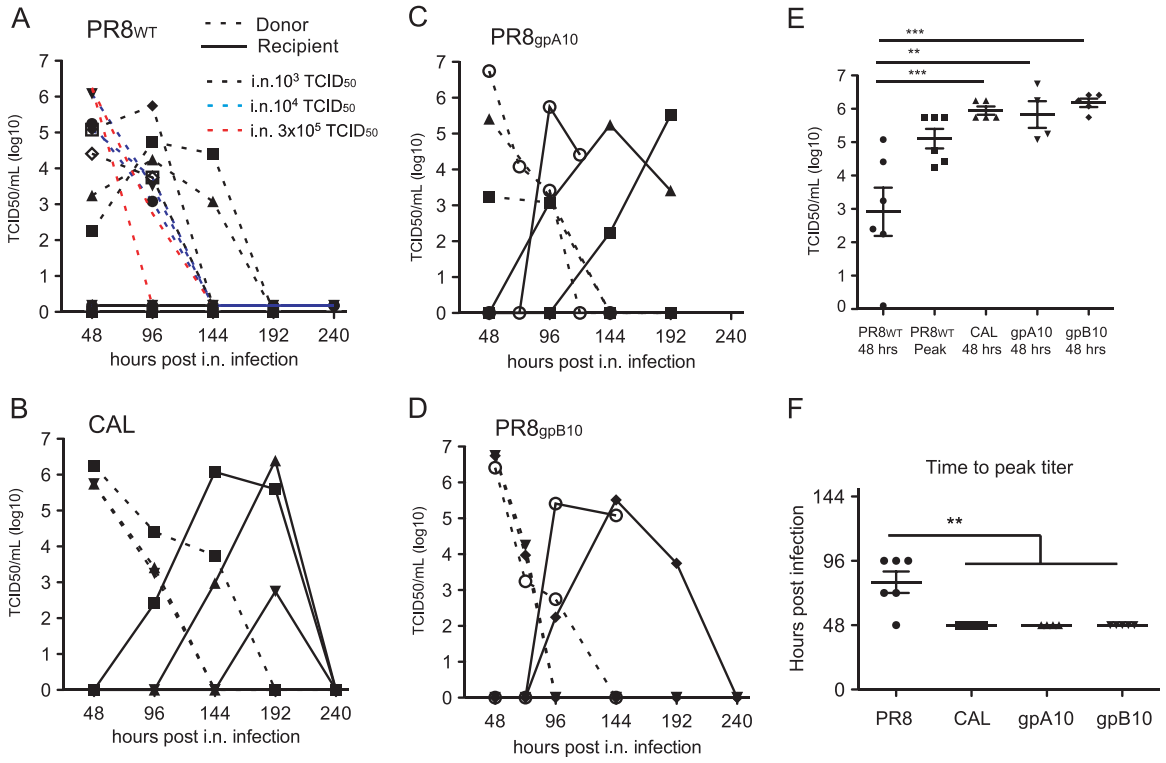

FIG 1 Replication and transmissibility of $PR8_{WT}$, CAL, and GP-adapted PR8 in GPs. Data are combined from multiple experiments. (A to D) Nasal wash titers of intranasally infected transmission donors (dashed lines) and naïve cocaged transmission recipients (solid lines). Donor-recipient pairs are identified by like symbols. (A) Nasal wash virus titers of 9 GPs intranasally infected with 10^3 (black) (4 GPs), 3×10^4 (blue) (3 GPs), or 3×10^5 (red) (2 GPs) $TCID_{50}$s of $PR8_{WT}$ and their naïve cage mates. (B) Nasal wash virus titers of 3 GPs intranasally infected with 10^3 $TCID_{50}$ of CAL and their naïve cage mates. $P = 0.028$ (Fisher's exact test) for differences between $PR8_{WT}$ and CAL in transmission efficiency at identical $TCID_{50}$s in the donor animal. (C and D) Open circles represent data from a different experiment in which nasal washes were performed at the alternative time points indicated. (C) Nasal wash virus titers of 3 transmission pairs with donors infected with 10^3 to 10^5 $TCID_{50}$s of $PR8_{gpA10}$ (gpA10). (D) Nasal wash titers of 3 transmission pairs with donors infected with 10^3 to 10^4 $TCID_{50}$s of $PR8_{gpB10}$ (gpB10). (E) Nasal wash titers at 48 h ($PR8_{WT}$, CAL, $PR8_{gpB10}$ [gpB10], and $PR8_{gpA10}$ [gpA10]) and peak titer ($PR8_{WT}$) for GPs infected with 10^3 $TCID_{50}$s of the indicated virus. (F) Time of peak titers for $PR8_{WT}$, CAL, and GP-adapted PR8 (gpA10 and gpB10). Titer data from appropriately dosed GPs depicted in panels A to D were included in the analysis in panels E and F in addition to data from animals infected but not cocaged for transmission tests. Means ± standard errors of the means are plotted. ***, $P < 0.001$; **, $P < 0.01$ (one-way analysis of variance).

Accumulation of nonsynonymous substitutions in NP. Unlike $PR8_{gpB}$, $PR8_{gpA}$ accumulated additional nonsynonymous substitutions in multiple genes between passages 3 and 10 (Fig. 2). Variability increased with passaging, with segment 5, encoding NP, exhibiting the greatest diversity. NP_{T378A} and NP_{F346S} emerged as minor variants by passages 3 and 5, respectively. By passage 10, these substitutions were joined by NP_{A336T} and NP_{M159I} in the population.

In the $PR8_{gpA10}$ population, we established intragenic linkage for NP substitutions A336T and M159I and found that the $NP_{M159I/A336T}$, NP_{F346S}, and NP_{T378A} substitutions were mutually exclusive (Fig. 2E and G). This, along with the clustering of these substitutions, both structurally and within a 44-amino-acid region, suggests functional similarity (see Discussion). Nonsynonymous mutations emerged in other genes, including NA_{K272R}, HA_{H130Y}, and linked substitutions $PB2_{Q194K}$ and $PB2_{T683I}$. Unlike variants of PB2, NA, and HA, which remained as minority species, NP variants arose early in passaging and jointly outcompeted the wild-type variant on the background of the M1 F62L in line A (Fig. 2A, C, and E) but not on the background of M1 V166M in line B. These findings imply relatively strong selection for these substitutions, and thus a role for NP in adaptation of PR8 to GPs, in the context of a subset of M1 substitutions.

Sequencing of 60 plaque clones revealed that the allelic variants of the PB2, HA, NP, and NA genes constituted at least 15 genotypes (combinations of alleles) (Fig. 2G), clearly demonstrating the high frequency of segment reassortment during GP passaging. The 6 most abundant genotypes comprised 72% of the population, and each ranged from 7 to 17% in frequency, indicating no strong selective advantage for any single assortant during serial nasal wash passaging.

Transmission of multiple minor variants from diverse donor populations. Which genotypes in the diverse $PR8_{gpA}$ population are best transmitted to naïve cage mates? Only the single genotype representing the prevalent virus in line B was transmitted to cage mates (Fig. 1D and 2F). In contrast, transmitted viruses replicating in GPs cocaged with $PR8_{gpA10}$-infected animals (Fig. 1C) consisted of distinct genotypes, both within and between recipient animals (Fig. 3). Importantly, all transmitted genotypes contained the $M1_{F62L}$ allele, the dominant allele in the donor input population (Fig. 2G). The genotypes that dominated in transmission recipients 101 and 102 (Fig. 3A and B) represented 3% or less of the $PR8_{gpA10}$ input population genotypes (Fig. 2G). Remarkably, both of these transmitted viruses possessed HA_{H130Y} and NA_{K272R} together despite their mutual exclusivity ($P < 0.001$) in the $PR8_{gpA10}$ population at peak titer (Fig. 2G). All variants sampled from re-

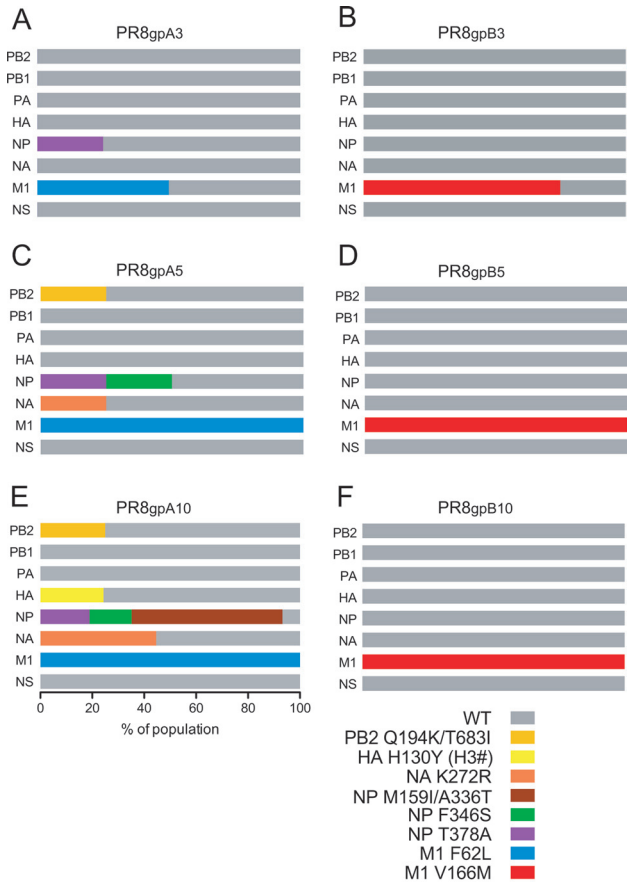

G

PB2 Q194K /T683I	HA H130Y	NP M159I /A336	NP F346S	NP T378A	NA K272R	M1 F62L	# of clones	%
							10	17
							10	17
							8	13
							6	10
							5	8
							4	7
							3	5
							3	5
							3	5
							2	3
							2	3
							1	2
							1	2
							1	2
							1	2

FIG 2 Frequency of nonsynonymous substitutions in passaged virus populations. (A to F) Stacked bar graphs indicate the relative proportions of variants (horizontal axis) defined by nonsynonymous substitutions (for HA, H3 numbering is used) for each gene segment (vertical axis) in the virus populations at different passages. Graphs without horizontal units reflect the approximate proportions of variants estimated from peak heights in sequence traces from bulk population sequencing, indicating major and minor variants or homogeneous populations (A to D and F). Where indicated, percentages of variants were estimated from sequencing of 60 plaque-cloned viruses (E and G). (A and B) passage 3; (C and D) passage 5; (E and F) passage 10. (A, C, and E) line A; (B, D, and F) line B. (G) Frequencies of genotypes containing specifc PB2, HA, NP, NA, and M1 alleles in the $PR8_{gpA10}$ population. Colored boxes indicate mutant alleles.

cipient 102 possessed an additional NA substitution, K250R, and a subset of clones (6/25) possessed a V591I substitution in PB1, which were not detected in the donor population (0/28 clones). Recipient 103 had a mixed population dominated by two genotypes: one with $PB2_{Q194K/T683I}$, HA_{H130Y}, and NP_{T378A} and one with NP_{F346S} and NP_{A284T}, an additional substitution not detected in the $PR8_{gpA10}$ input population.

Together, these data indicate the following: (i) the multiple variants that appear during serial GP nasal wash passaging are capable of transmission, (ii) minor and even undetected genotypic variants can be transmitted from the donor population, and (iii) multiple variants can be transmitted to a single recipient during cohabitation, indicating a relatively wide bottleneck.

Reassortment between IAV lines A and B generates a fitter transmissible virus. Given the distinct evolutionary pathways exhibited by $PR8_{gpA}$ and $PR8_{gpB}$ viruses, which is fitter in GPs? Passaging a 1:1 mixture of the two populations for 10 rounds (generating the $PR8_{gpAB20}$ virus) resulted in genotypes carrying the $M1_{V166M}$ allele (29/32 clones) outcompeting those carrying $M1_{F62L}$ (3/32 clones) (Fig. 4A and B) and the emergence of a major set of genotypes (17/32 clones) encoding both $M1_{V166M}$ and NP_{F346S}, presumably a result of reassortment between preexisting variants in $PR8_{gpA10}$ and $PR8_{gpB10}$ (Fig. 4B). We did not detect the $PR8_{gpA10}$ allelic variants $NP_{M159I/A336T}$, NP_{T378A}, HA_{H130Y}, and NA_{K272R}, but we found a novel substitution, $PB2_{T521I}$, in a substantial fraction of clones (14/32) in combination with NP_{F346S}, $M1_{V166M}$, and $M1_{F62L}$ variants in the $PR8_{gpAB20}$ population.

Importantly, $PR8_{gpAB20}$-derived viruses maintained their ability to transmit to naïve cage mates (Fig. 4C) and demonstrated increased fitness relative to $PR8_{gpA10}$ viruses in coinfected animals (Fig. 5). Virus sampled from the 4 transmission recipients cocaged with donors infected with $PR8_{gpAB20}$ (Fig. 4D to G) represented 2 of the 6 genotypic variants detected in the $PR8_{gpAB20}$ donor input population (Fig. 4B). Transmitted variants contained NP_{F346S} and $M1_{V166M}$, either with (1) or without (3) $PB2_{T521I}$ (Fig. 4D to G). When we mixed $PR8_{gpAB20}NP_{F346S}M1_{V166M}$ approximately 1:1 in donor animals with either of two clonal variants ($PR8_{gpA10.101}$ or $PR8_{gpA10.102}$) transmitted from the $PR8_{gpA10}$ population (Fig. 3A and B), $PR8_{gpAB20}NP_{F346S}M1_{V166M}$ rapidly outcompeted the $PR8_{gpA10}$-derived viruses in infectivity and replication (Fig. 5). While we detected reassortment between competing viruses, we found that viruses possessing the $PR8_{gpAB20}$-derived NP_{F346S} and $M1_{V166M}$ allelic variants exhibited a distinct fitness advantage over those with the $PR8_{gpA10}$-derived NP and M1 variants (Table 1). In the 3 transmission events for which a genotype could be determined (adequate genotype data could not be obtained for the transmission recipient paired with GP 1B, which had the lowest virus titer), virus with the complete $PR8_{gpAB20}NP_{F346S}M1_{V166M}$ genotype was transmitted in 2 cases, but in 1 case, the transmitted virus was a reassortant containing the $PR8_{gpA10}$-derived $PB1_{V591I}$, HA_{H130Y}, $NA_{K250R/K272R}$, and $NP_{M159I/A336T}$ allelic variants along with the $PR8_{gpAB20}$-derived $M1_{V166M}$ variant (Fig. 5).

Together, these data are consistent with increased fitness, conferred specifically by the allelic variants NP_{F346S} and $M1_{V166M}$, as the basis for the dominance of $PR8_{gpAB20}$ variants over $PR8_{gpA10}$ variants in the passage 20 virus population, as opposed to stochastic effects.

Mutations in either NP or M1 increase viral replication and transmissibility and are selected for their combined effect. Both the $M1_{F62L}$ (in $PR8_{gpA}$) and the $M1_{V166M}$ (in $PR8_{gpB}$) substitutions

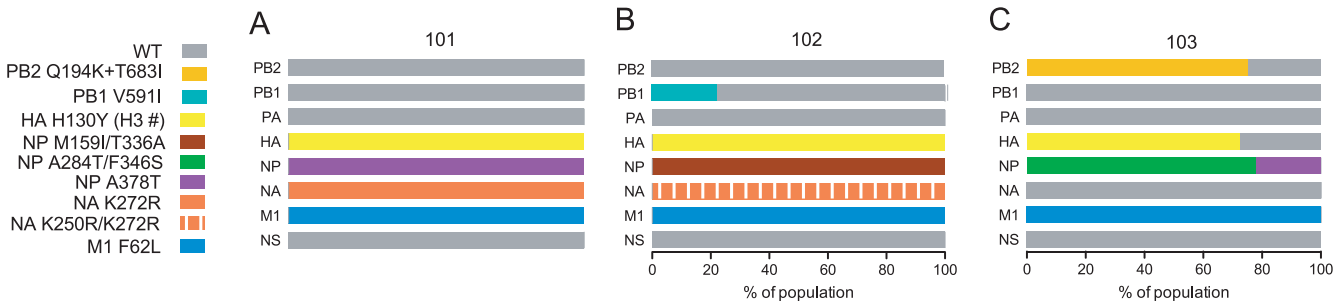

FIG 3 Transmitted $PR8_{gpA10}$ virus variant frequency in transmission recipients. The genotypes of viruses from transmission recipients cocaged with GPs infected with the $PR8_{gpA10}$ virus population (Fig. 1C) are depicted. Stacked bar graphs indicate the relative proportions of variants (horizontal axis) defined by nonsynonymous substitutions (for HA, H3 numbering is used) for each gene segment (vertical axis) in the $PR8_{gpA10}$ transmitted virus populations (see Fig. 2G for $PR8_{gpA10}$ variant frequencies in the donor population). (A) Bulk sequencing indicated a homogeneous population in animal 101, which was cocaged with a GP inoculated with 10^3 $TCID_{50}$s of $PR8_{gpA10}$. (B and C) Percentages of variants were estimated from sequencing of 24 plaque-cloned viruses (in addition to bulk sequencing). GPs 102 and 103 were cocaged with GPs infected with 10^5 $TCID_{50}$s of $PR8_{gpA10}$.

alone conferred transmissibility when reintroduced singly into the wild-type background by reverse genetics (Fig. 6 A and B). However, $M1_{V166M}$, together with NP_{F346S}, outcompeted $M1_{F62L}$ when passages were combined (Fig. 4). In order to determine the relative contributions of NP_{F346S} and $M1_{V166M}$ to IAV GP replication and transmission, we generated molecular-clone-derived single mutants. NP_{F346S} and $M1_{V166M}$ substitutions each conferred transmissibility, as did the $NP_{F346S}/M1_{V166M}$ double mutant (Fig. 6B to D). Single mutants also conferred more rapid and robust growth kinetics relative to $PR8_{WT}$ virus ($P < 0.01$) but were not clearly distinguishable from the double mutant by this measure (Fig. 6E). Thus, a growth and transmissibility advantage in guinea pigs can be conferred by a single mutation encoding an amino acid substitution in either NP or M1.

In order to maximize sensitivity to detect differences in relative transmissibility between the single and double mutants, we infected GPs with a mixture of the single NP_{F346S} and $M1_{V166M}$ mutants at a 1:1 ratio. Each of 6 animals, infected intranasally (i.n.) with the mutant mixture, was then cocaged 1:1 with naïve GPs. Three of the 6 infected animals transmitted to naïve cage mates (Fig. 7A). In each case, the transmitted virus was the reassortant $NP_{F346S}/M1_{V166M}$ double mutant (the lack of transmission between 3 pairs may reflect the 50% transmission efficiency of these variants when directly competing with each other). Analysis of cloned viruses isolated from three of the donor animals (two transmitters and one nontransmitter) (Fig. 7B) revealed that the double mutant was generated in the donor and was represented at 18 to 43% at peak titer in these animals, indicating a selective advantage in growth and transmission for this combination of alleles over the single mutants alone. Interestingly, the reciprocal reassortant, wild-type (WT) PR8, was also detected at 6 to 14%, consistent with the idea that a large number of independent reassortment events may have contributed to the observed frequencies of both the WT and double mutant viruses, rather than relative growth advantage alone. This also demonstrates that substantially less fit viruses generated by reassortment can arise and persist in an infection, if not be transmitted. Together, these results demonstrate a positive interaction between NP_{F346} and $M1_{V166M}$ in increasing fitness and highlight the advantage of a segmented genome in accelerating viral adaptation to a new host.

DISCUSSION

Understanding IAV host adaptation requires studying multiple virus strains in multiple animal infection models. Thanks to the Palese laboratory, the GP has been rediscovered and developed as a robust model of IAV transmission (11, 13, 14). In this study, we have explored IAV evolutionary dynamics during serial passaging and transmission of mouse-adapted PR8 in GPs. Our major finding is that while the virus samples multiple genetic pathways during adaptation, mutations in the NP and M1 genes are central to increasing GP replication and transmission of PR8 and further implicate these genes in host adaptation in general.

PR8, which has a long and varied passage history in laboratory mice, embryonated chicken eggs, and immortalized canine cells, does not replicate well and is not transmitted in GPs, unlike other IAVs isolated from humans or other mammals (23, 24, 28). PR8 therefore provides a unique angle to probe the genetics of host adaptation, particularly mammal-to-mammal adaptation, since most studies examine adaptation of avian viruses to mammals (29).

The M1 gene is a known determinant of IAV respiratory droplet transmission in GPs, based on studies with reassortant virus expressing the M1 gene of the 2009 swine origin H1N1 (SOIV) virus on the background of PR8 genes (22). Recent outbreaks in humans of variant swine H3N2 viruses containing the M1 gene of the 2009 SOIV confirm the critical role of this gene in host adaptation and transmission (26). We extend these findings by demonstrating that GP replication and transmission are enhanced by F62L or V166M substitutions in M1. While some distance separates these substitutions in the linear sequence, their physical relationship remains unclear due to a lack of structural information. Neither of these residues is among the 13 residues that differ between the 2009 SOIV and PR8 M1 proteins, although the V167A in SOIV M1 may function similarly based on proximity and similarity to V166M.

We found that mutations in NP alone play a significant role in GP adaptation of PR8, extending findings from mouse adaptation studies of human SOIV and avian viruses pointing to a contribution from NP in determining host specificity (30, 31). All the NP substitutions we identified (except M159I, which is linked to A336T) cluster in a region thought to influence NP-PB2 interactions (27, 32), suggesting a common function. While all NP sub-

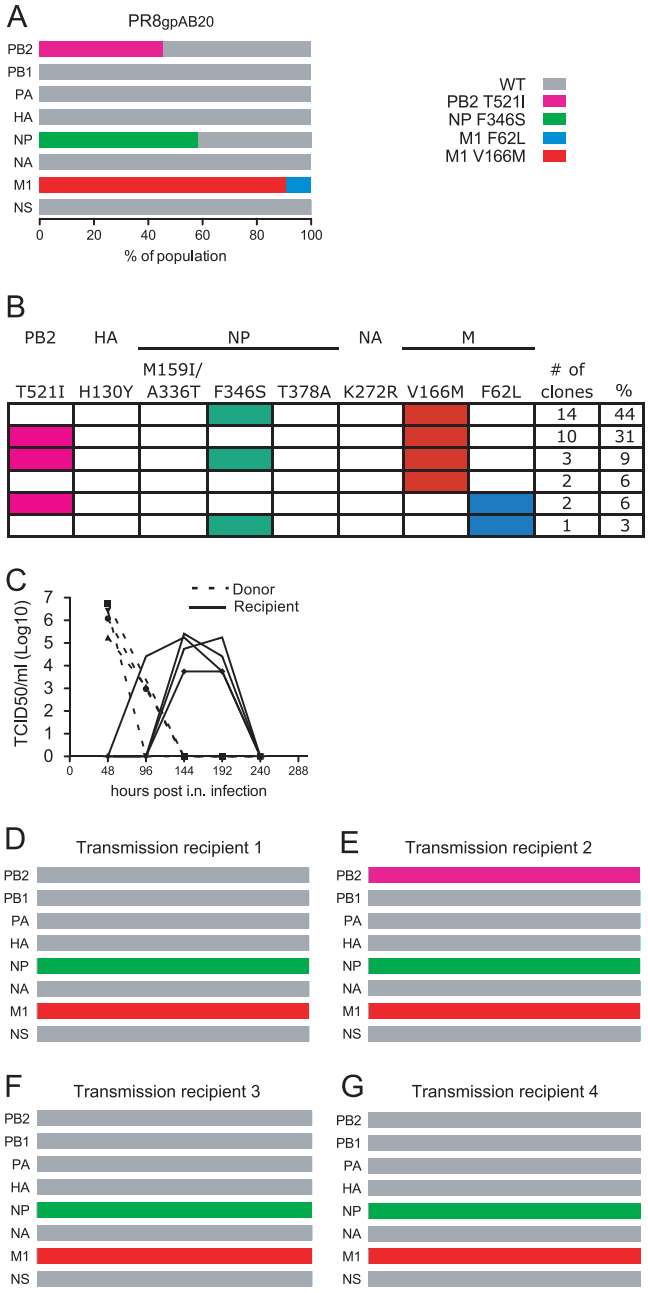

FIG 4 Transmission of variants from $PR8_{gpAB20}$-infected animals. (A and B) Mutant allele frequencies (A) and frequency of genotypes containing specific allele combinations (B) in the $PR8_{gpAB20}$ inoculum were determined by sequencing 32 plaque-cloned viruses. (C) Four animals infected with 1×10^4 $TCID_{50}$s of $PR8_{gpAB20}$ (dashed lines) cocaged with naïve recipients (solid lines). (D to G) Mutation frequencies in virus from transmission recipients cocaged with $PR8_{gpAB20}$-infected animals. (A and D to G) Stacked bar graphs indicate the relative proportions of variants (horizontal axis) defined by nonsynonymous substitutions for each gene segment (vertical axis) in the virus populations. Graphs without horizontal units reflect the approximate proportions of variants estimated from peak heights in sequence traces from bulk population sequencing, indicating major and minor variants or homogeneous populations.

stitutions are at highly conserved positions in natural isolates, A336T and F346S in particular are adjacent to variable positions. Gabriel and colleagues found that N319K, which is physically proximal to GP adaptation-associated residues A336T, F346L, and T378A, is associated with mouse adaptation and modulates polymerase activity through interaction with host importin-alpha isoforms (30, 33). NP has also been implicated in Mx protein sensitivity (34). Addressing the mechanisms underlying M1 and NP adaptation to GPs is clearly an important area of future research.

The difference in evolutionary rates in line A and B passage populations is intriguing. Line A, which acquired and fixed the $M1_{F62L}$ substitution early, continued to accumulate substitutions in other genes, most notably in the NP gene. In contrast, line B acquired and fixed $M1_{V166M}$ early but did not accumulate additional substitutions. One explanation for this observation is that line B experienced more severe bottlenecks during passaging. While lines A and B were initiated with 10^5 and 10^6 $TCID_{50}$s, respectively, in the first 5 passages, line A infectious dosing did not drop below 5×10^4, whereas at passage 2 the line B dose dropped to 5×10^3. Even at this lower dose, however, we expect to sample any variant at >0.1% in the population. Alternatively, the virus carrying the $M1_{V166M}$ allelic variant, which outcompeted the $M1_{F62L}$ allelic variant in both passaging (Fig. 4A) and the repeated-competition experiment (Fig. 5), may be at a fitness peak where additional mutations are more likely to be detrimental or nearly neutral, slowing further evolution. To make this conclusion requires additional experiments that gauge the effects of further mutations on the fitness of each virus lineage.

High and variable rates of reassortment between competing viruses, and a dynamic environment (e.g., finite numbers of susceptible cells, selective pressures at the point of initial infection may be distinct from those later on, etc.), complicate the interpretation of our estimations of relative fitness measurements in Table 1. While we expect beneficial alleles to dominate over the course of passaging, obtaining fitness estimations for a given allele, or genotype, that accurately predict the time to fixation over multiple passages may not be pragmatically possible in this context. Instead, our fitness estimations in Table 1 are intended to demonstrate, roughly, the relative fitness advantage that one allele or set of alleles has over another in the course of a 48-h infection. For example, in spite of the $M1_{V166M}$ mutant exhibiting a distinct growth advantage over $M1_{F62L}$ (Fig. 4A and 5), the former does not become fixed at 100% over 10 guinea pig passages. We believe that while this means that $M1_{V166M}$ is the fittest allele in the course of a single infection, we are not accounting for all the selective pressures present during passaging or the effect that reassortment with a competing virus has on allele frequency in a dynamic environment. This is most strikingly demonstrated in the data illustrated in Fig. 7B, which shows the spontaneously generated WT PR8 genotype is present at 6 to 14% in the population in spite of exhibiting a substantial growth defect in guinea pigs (Fig. 6E) and disappearing within 5 guinea pig passages (Fig. 2C and D).

Efficient recombination through genome segment reassortment greatly enhances IAV evolution by combining preexisting beneficial mutations that have additive or synergistic effects on fitness. While no additional substitutions appeared in line B after the fixation of $M1_{V166M}$, when line A and B viruses were copassaged, the line A substitution NP_{F346S} combined with $M1_{V166M}$ from line B, increasing fitness of the resulting reassortant (Fig. 4B and Table 1), which outcompeted each single-mutant parent during transmission (Fig. 7). This combination of alleles may have been unlikely to have reached fixation in the absence of reassortment if a spontaneously generated double mutant lacked a large

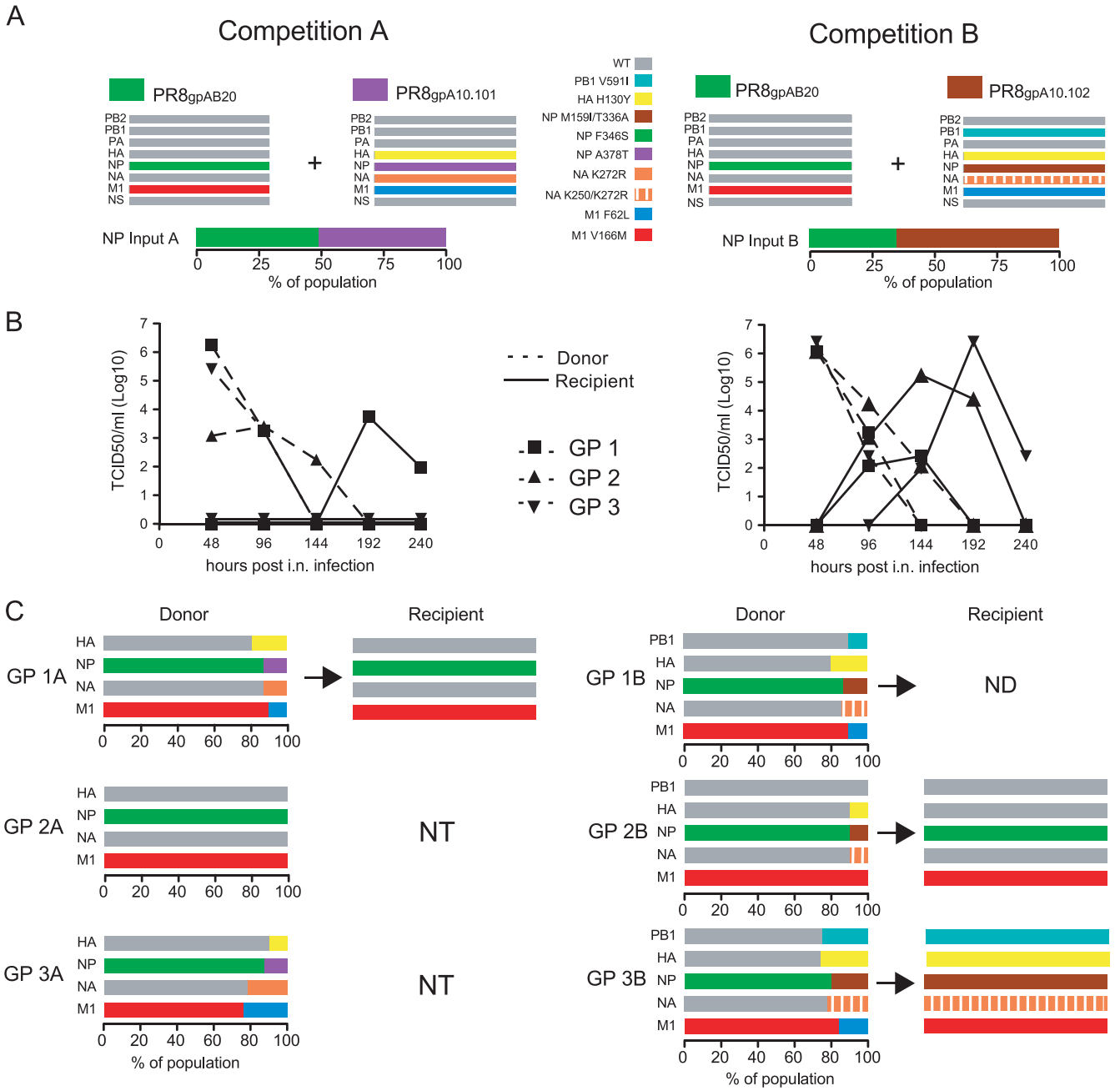

FIG 5 Replication and transmission advantage of $PR8_{gpAB20}$-derived genotypic variants compared to $PR8_{gpA10}$ variants. (A) Selected $PR8_{gpA10}$ and $PR8_{gpAB20}$ transmitted variants included in 2 mixtures, "competition A" (left side) and "competition B" (right side), and their relative frequencies of NP allelic variants measured in the input mixtures. (B) Nasal wash virus titers of donor animals (dashed lines) infected with 4,000 $TCID_{50}$s of competition A (left) or B (right) virus mixture and their naïve cage mates (solid lines). Like symbols indicate transmission pairs. (C) Frequencies of allelic variants in competition A donors (left) and competition B donors (right), at 48 h postinfection, and the genotypes of transmitted viruses from the recipient guinea pigs in each transmission pair. NT, no transmission; ND, not determined.

enough fitness advantage to overcome the frequency threshold to be carried forward, greater than 0.1% in nasal wash passaging and likely much higher for natural transmission. However, as illustrated in Fig. 7B, multiple *in vivo* reassortment events between two single mutants resulted in double mutants appearing at >20% at peak titer and allowed for transmission of the double mutant reassortant. Thus, this model emphasizes the role of reassortment, in complementing spontaneous mutation, as a key feature of IAV adaptability.

The transmission of multiple variants, observed in this study and in other transmission models (35–38), suggests that the transmission bottleneck in IAV may not be so severe in many circumstances, which would enhance the diversity on which selection can act in transmission recipients. The mode of transmission likely impacts the size of the bottleneck. In a "contact transmission" model described here, all modes of transmission, from direct contact with nasal secretions to aerosolized virus, can contribute to transmission (imagine child day care), with each mode potentially

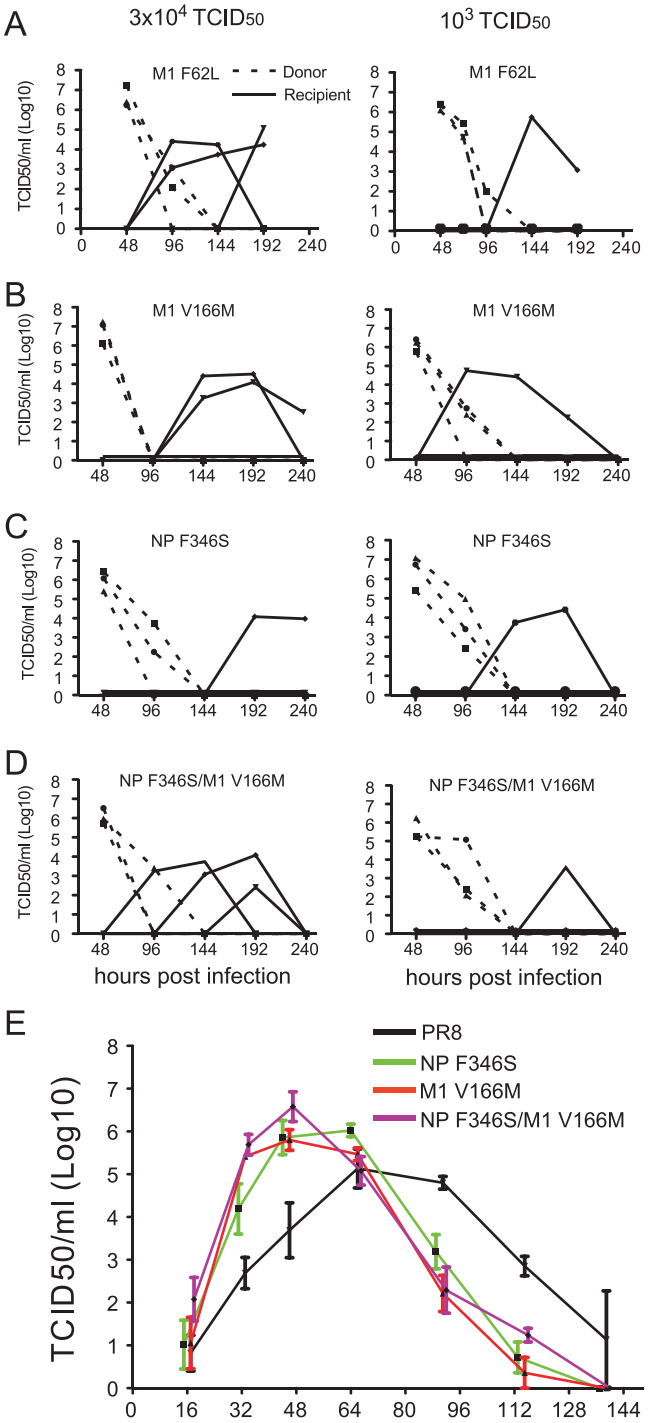

FIG 6 Replication kinetics and transmissibility of M1 and NP single and double mutants. (A to D) Nasal wash virus titers of GPs intranasally infected (dashed lines) and their naïve cage mates (solid lines). Three donor GPs were infected with 3×10^4 (left panels) or 10^3 (right panels) $TCID_{50}$s of the molecular-clone-derived mutants $M1_{F62L}$ (A), $M1_{V166M}$ (B), NP_{F346S} (C), or $NP_{F346S}/M1_{V166M}$ (D). (E) Nasal wash virus titers of animals infected with 500 $TCID_{50}$s of molecular-clone-derived PR8 (black line), the $NP_{F346S}/M1_{V166M}$ double mutant (purple line), the NP_{F346S} single mutant (green line), or the $M1_{V166M}$ single mutant (red line). Means ± standard errors of the means of 3 replicates are plotted. A two-way analysis of variance was used to test the significance of differences in virus titers over the course of sampling (see Results).

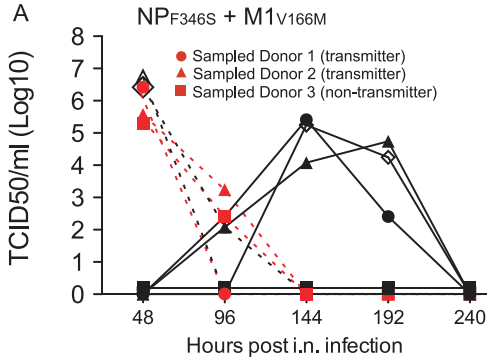

B

NP F346S	M1 V166M	Input	Transmitters: Donor 1	Donor 2	Donor 3	Transmitted virus
■		76	6	7	50	0/3
	■	24	47	36	18	0/3
■	■	0	41	43	18	3/3
		0	6	14	14	0/3

FIG 7 Reassortment between NP_{F346S} and $M1_{V166M}$ single mutants produces a dominantly transmitting double mutant. (A) Nasal wash virus titers of 6 GPs intranasally infected with 3×10^4 each of the NP_{F346S} and $M1_{V166M}$ single mutants (dashed lines) and their naïve cage mates (solid lines). (B) Genotype frequencies in the input virus, virus sampled from indicated inoculated animals in panel A at 48 h (2 of 3 transmitters and 1 of 3 nontransmitters, indicated by red symbols), and their transmission recipients, which had homogeneous populations. Colored cells indicate mutant alleles. Frequencies of genotypes in donor animals were estimated from sequencing 34 (input), 17 (donor 1), 14 (donor 2), and 22 (donor 3) plaque-cloned viruses.

delivering different doses of virus or viruses with different biological properties. In addition, multiple variants can be transmitted to the recipient animals either in a "single" transmission event or sequentially over several hours of cohabitation. In either case, the transmission of diversity may allow variants with moderate fitness advantages to emerge and grow out over the course of multiple transmission events. Preexisting immunity in guinea pigs has been shown to impact virus evolution during the course of a single infection (39), which raises the possibility of modeling in GPs viral evolution during transmission to animals with various states of preexisting immunity, as has been demonstrated in swine, horses, and dogs (36, 37, 40).

The clear advantages of reassortment as an evolutionary accelerant may create a perfect storm for human IAV evolution in young children. Their naturally low hygiene likely results in transmission of higher doses with concomitant increases in genetic diversity. In combination with multiple contacts in a day care or school setting, children could be the primary source of highly adapted viruses. This is potentially one more reason for focusing efforts on increasing childhood IAV vaccination.

ACKNOWLEDGMENTS

This work was supported by the Division of Intramural Research, NIAID, and funds provided by the American Recovery and Reinvestment Act.

We are grateful to James Magrath, Alfonso Gozalo, and the NIAID Comparative Medicine Branch for technical assistance.

REFERENCES

1. **Dugan VG, Chen R, Spiro DJ, Sengamalay N, Zaborsky J, Ghedin E, Nolting J, Swayne DE, Runstadler JA, Happ GM, Senne DA, Wang R, Slemons RD, Holmes EC, Taubenberger JK.** 2008. The evolutionary

genetics and emergence of avian influenza viruses in wild birds. PLoS Pathog. **4**:e1000076. doi:10.1371/journal.ppat.1000076.
2. **Olsen B, Munster VJ, Wallensten A, Waldenstrom J, Osterhaus AD, Fouchier RA.** 2006. Global patterns of influenza A virus in wild birds. Science **312**:384–388.
3. **Webster RG, Bean WJ, Gorman OT, Chambers TM, Kawaoka Y.** 1992. Evolution and ecology of influenza A viruses. Microbiol. Rev. **56**:152–179.
4. **Brown IH.** 2000. The epidemiology and evolution of influenza viruses in pigs. Vet. Microbiol. **74**:29–46.
5. **Smith GJ, Vijaykrishna D, Bahl J, Lycett SJ, Worobey M, Pybus OG, Ma SK, Cheung CL, Raghwani J, Bhatt S, Peiris JS, Guan Y, Rambaut A.** 2009. Origins and evolutionary genomics of the 2009 swine-origin H1N1 influenza A epidemic. Nature **459**:1122–1125.
6. **Jagger BW, Wise HM, Kash JC, Walters KA, Wills NM, Xiao YL, Dunfee RL, Schwartzman LM, Ozinsky A, Bell GL, Dalton RM, Lo A, Efstathiou S, Atkins JF, Firth AE, Taubenberger JK, Digard P.** 2012. An overlapping protein-coding region in influenza A virus segment 3 modulates the host response. Science **337**:199–204.
7. **Palese P, Shaw M.** 2007. Orthomyxoviridae: the viruses and their replication, p 1647–1689. *In* Knipe DM, Howley PM, Griffin DE, Lamb RA, Martin MA, Roizman B, Straus SE (ed), Fields virology, 5th ed, vol 2. Lippincott Williams & Wilkins, Philadelphia, PA.
8. **Suárez P, Valcarcel J, Ortin J.** 1992. Heterogeneity of the mutation rates of influenza A viruses: isolation of mutator mutants. J. Virol. **66**:2491–2494.
9. **Medina RA, Garcia-Sastre A.** 2011. Influenza A viruses: new research developments. Nat. Rev. Microbiol. **9**:590–603.
10. **Barnard DL.** 2009. Animal models for the study of influenza pathogenesis and therapy. Antiviral Res. **82**:A110–A122. doi:10.1016/j.antiviral.2008.12.014.
11. **Bouvier NM, Lowen AC.** 2010. Animal models for influenza virus pathogenesis and transmission. Viruses **2**:1530–1563.
12. **O'Donnell CD, Subbarao K.** 2011. The contribution of animal models to the understanding of the host range and virulence of influenza A viruses. Microbes Infect. **13**:502–515.
13. **Bouvier NM, Lowen AC, Palese P.** 2008. Oseltamivir-resistant influenza A viruses are transmitted efficiently among guinea pigs by direct contact but not by aerosol. J. Virol. **82**:10052–10058.
14. **Lowen AC, Mubareka S, Tumpey TM, Garcia-Sastre A, Palese P.** 2006. The guinea pig as a transmission model for human influenza viruses. Proc. Natl. Acad. Sci. U. S. A. **103**:9988–9992.
15. **Lowen AC, Steel J, Mubareka S, Carnero E, Garcia-Sastre A, Palese P.** 2009. Blocking interhost transmission of influenza virus by vaccination in the guinea pig model. J. Virol. **83**:2803–2818.
16. **Martinez-Sobrido L, Garcia-Sastre A.** 2010. Generation of recombinant influenza virus from plasmid DNA. J. Vis. Exp. **42**:e2057. doi:10.3791/2057.
17. **Vallejo AN, Pogulis RJ, Pease LR.** 2008. PCR mutagenesis by overlap extension and gene SOE. CSH Protoc. **2008**:pdb.prot4861. doi:10.1101/pdb.prot4861.
18. **Szretter KJ, Balish AL, Katz JM.** 2006. Influenza: propagation, quantification, and storage. Curr. Protoc. Microbiol. **3**:15G.1.1–15G.1.22. doi:10.1002/0471729256.mc15g01s3.
19. **Zhou B, Wentworth DE.** 2012. Influenza A virus molecular virology techniques. Methods Mol. Biol. **865**:175–192.
20. **Gerber P, Loosli CG, Hambre D.** 1955. Antigenic variants of influenza A virus, PR8 strain. I. Their development during serial passage in the lungs of partially immune mice. J. Exp. Med. **101**:627–638.
21. **Quilligan JJ, Jr, Minuse E, Francis T, Jr.** 1948. Homologous and heterologous antibody response of infants and children to multiple injections of a single strain of influenza virus. J. Clin. Invest. **27**:572–579.
22. **Chou YY, Albrecht RA, Pica N, Lowen AC, Richt JA, Garcia-Sastre A, Palese P, Hai R.** 2011. The M segment of the 2009 new pandemic H1N1 influenza virus is critical for its high transmission efficiency in the guinea pig model. J. Virol. **85**:11235–11241.
23. **Steel J, Staeheli P, Mubareka S, Garcia-Sastre A, Palese P, Lowen AC.** 2010. Transmission of pandemic H1N1 influenza virus and impact of prior exposure to seasonal strains or interferon treatment. J. Virol. **84**:21–26.
24. **Sun Y, Bi Y, Pu J, Hu Y, Wang J, Gao H, Liu L, Xu Q, Tan Y, Liu M, Guo X, Yang H, Liu J.** 2010. Guinea pig model for evaluating the potential public health risk of swine and avian influenza viruses. PLoS One **5**:e15537. doi:10.1371/journal.pone.0015537.
25. **Hanley JA, Lippman-Hand A.** 1983. If nothing goes wrong, is everything all right? Interpreting zero numerators. JAMA **249**:1743–1745.
26. **Centers for Disease Control and Prevention.** 2012. Update: influenza A (H3N2)v transmission and guidelines—five states, 2011. MMWR Morb. Mortal. Wkly. Rep. **60**:1741–1744.
27. **Biswas SK, Boutz PL, Nayak DP.** 1998. Influenza virus nucleoprotein interacts with influenza virus polymerase proteins. J. Virol. **72**:5493–5501.
28. **Leyva-Grado VH, Mubareka S, Krammer F, Cárdenas WB, Palese P.** 2012. Influenza virus infection in guinea pigs raised as livestock, Ecuador. Emerg. Infect. Dis. doi:10.3201/eid1807.111930.
29. **Reperant LA, Kuiken T, Osterhaus AD.** 2012. Adaptive pathways of zoonotic influenza viruses: from exposure to establishment in humans. Vaccine **30**:4419–4434.
30. **Gabriel G, Herwig A, Klenk HD.** 2008. Interaction of polymerase subunit PB2 and NP with importin alpha1 is a determinant of host range of influenza A virus. PLoS Pathog. **4**:e11. doi:10.1371/journal.ppat.0040011.
31. **Sakabe S, Ozawa M, Takano R, Iwastuki-Horimoto K, Kawaoka Y.** 2011. Mutations in PA, NP, and HA of a pandemic (H1N1) 2009 influenza virus contribute to its adaptation to mice. Virus Res. **158**:124–129.
32. **Li Z, Watanabe T, Hatta M, Watanabe S, Nanbo A, Ozawa M, Kakugawa S, Shimojima M, Yamada S, Neumann G, Kawaoka Y.** 2009. Mutational analysis of conserved amino acids in the influenza A virus nucleoprotein. J. Virol. **83**:4153–4162.
33. **Gabriel G, Klingel K, Otte A, Thiele S, Hudjetz B, Arman-Kalcek G, Sauter M, Shmidt T, Rother F, Baumgarte S, Keiner B, Hartmann E, Bader M, Brownlee GG, Fodor E, Klenk HD.** 2011. Differential use of importin-alpha isoforms governs cell tropism and host adaptation of influenza virus. Nat. Commun. **2**:156.
34. **Zimmermann P, Manz B, Haller O, Schwemmle M, Kochs G.** 2011. The viral nucleoprotein determines Mx sensitivity of influenza A viruses. J. Virol. **85**:8133–8140.
35. **Hurt AC, Nor'e SS, McCaw JM, Fryer HR, Mosse J, McLean AR, Barr IG.** 2010. Assessing the viral fitness of oseltamivir-resistant influenza viruses in ferrets, using a competitive-mixtures model. J. Virol. **84**:9427–9438.
36. **Murcia PR, Baillie GJ, Daly J, Elton D, Jervis C, Mumford JA, Newton R, Parrish CR, Hoelzer K, Dougan G, Parkhill J, Lennard N, Ormond D, Moule S, Whitwham A, McCauley JW, McKinley TJ, Holmes EC, Grenfell BT, Wood JL.** 2010. Intra- and interhost evolutionary dynamics of equine influenza virus. J. Virol. **84**:6943–6954.
37. **Murcia PR, Hughes J, Battista P, Lloyd L, Baillie GJ, Ramirez-Gonzalez RH, Ormond D, Oliver K, Elton D, Mumford JA, Caccamo M, Kellam P, Grenfell BT, Holmes EC, Wood JL.** 2012. Evolution of an Eurasian avian-like influenza virus in naive and vaccinated pigs. PLoS Pathog. **8**:e1002730. doi:10.1371/journal.ppat.1002730.
38. **Seibert CW, Kaminski M, Philipp J, Rubbenstroth D, Albrecht RA, Schwalm F, Stertz S, Medina RA, Kochs G, Garcia-Sastre A, Staeheli P, Palese P.** 2010. Oseltamivir-resistant variants of the 2009 pandemic H1N1 influenza A virus are not attenuated in the guinea pig and ferret transmission models. J. Virol. **84**:11219–11226.
39. **Long J, Bushnell RV, Tobin JK, Pan K, Deem MW, Nara PL, Tobin GJ.** 2011. Evolution of H3N2 influenza virus in a guinea pig model. PLoS One **6**:e20130. doi:10.1371/journal.pone.0020130.
40. **Hoelzer K, Murcia PR, Baillie GJ, Wood JL, Metzger SM, Osterrieder N, Dubovi EJ, Holmes EC, Parrish CR.** 2010. Intrahost evolutionary dynamics of canine influenza virus in naive and partially immune dogs. J. Virol. **84**:5329–5335.